Electronic Supplementary Information (ESI)

for

An artificial metallolyase with pliable 2-his-1-carboxylate facial triad for stereoselective Michael addition

Ryusei Matsumoto,[1] Saho Yoshioka,[2] Miho Yuasa,[2] Yoshitsugu Morita,[1] Genji Kurisu[3] and

Nobutaka Fujieda[1,2*]

[1]Department of Applied Biological Chemistry, Graduate School of Agriculture, Osaka Metropolitan University, 1-1 Gakuen-cho, Naka-ku, Sakai-shi, Osaka 599-8531, Japan, [2] Department of Applied Life Sciences, Graduate School of Life and Environmental Sciences, Osaka Prefecture University, 1-1 Gakuen-cho, Naka-ku, Sakai-shi, Osaka 599-8531, Japan, [3]Institute for Protein Research, Osaka University, 3-2 Yamada-oka, Suita, Osaka 565-0871, Japan.

Experimental Procedure

General: The reagents and the solvents used in this study are commercially available and were used without further purification. High resolution mass spectra were recorded on a linear mode of time-of-flight mass spectrometer (micrOTOF II, Bruker Daltonics). ESI-Mass spectra were obtained on an Agilent LC/MSD (G6125B) system. NMR spectra (JNM-ECZ R series, JEOL RESONANCE) were recorded at 500 MHz and tetramethylsilane was used as internal standard for ^{1}H and ^{13}C nuclei. The chemical shifts (δ) and coupling constants (*J*) were expressed in ppm and Hz, respectively. Chiral HPLC analyses were performed in a chromatograph (1260 Infinty II, Agilent Technologies, Inc.) equipped with a UV diode-array detector and polarimetric detector (OR-2090, JASCO Corp.) using chiral stationary columns from YMC Co., Ltd and DAICEL Co., Ltd. Retention times are given in minutes. The metal content was determined by an ICP-AES on ICPS-8100 apparatus (Shimadzu Corp.). Calibration curves of the metal ion used in this study were made by using the metal ion standard solution (10 ppm).

Plasmids, Site-directed Mutagenesis, and Expression and Purification of Proteins: For expression of TM1459 protein with Strep-tag, the pET30-based expression constructs were used as previously reported.[1] Oligonucleotide-directed mutagenesis experiments for introducing site-directed mutation were performed on the expression vector that contained the DNA fragment of TM1459. The pair of approximately 30 nucleotide long mutagenic oligonucleotides was purchased from Macrogen Japan Co (Table S4). The site-directed mutagenesis was carried out by inverse PCR, followed by DpnI digestion and self-ligation. For the mutant, the absence of undesired mutations on the gene was confirmed by DNA sequencing using 3730xl DNA Analyzer (Applied Biosystems) after the construction of the vector. The protein purification of wild type TM1459 and mutants thereof was conducted as described previously.[1,2] The fractions containing the TM1459 were collected and concentrated by ultrafiltration using Vivaspin turbo 15 (Sartorius AG). The protein samples were stored at –80 °C until use. Purity was determined by SDS-PAGE (Figure S1). Protein concentration was determined by measuring the intensity of absorbance at 280 nm.[3]

Crystallization: The purified apo-TM1459 protein (metal-depleted form) solution was desalted and exchanged to 10 mM HEPES buffer (pH 7.0) using PD-10 column (Cytiva). Then, an aliquot of an aqueous solution of $CuSO_4$ (300 μM, 1.5 equiv. for protein) was added to 200 μM apo-TM1459 protein solution under N_2. After incubation at 20 °C for 16 h, the resultant solution was loaded on PD-10 columns pre-equilibrated with 10 mM HEPES buffer (pH 7.0). The loaded sample was then eluted by the same buffer solution in order to remove excess amount of the metal. The collected fractions were concentrated up to 15 mg/mL by ultrafiltration using Vivaspin

turbo 15 and stored −80 °C until use. Cu-bound TM1459 were crystallized by hanging drop vapor diffusion method as previously described with some modification.[1,2] Crystallization drops were prepared by mixing the 0.1 M MES buffer at pH 6.0 containing 28 % w/v Jeffamine ED-2001 as precipitants (1 μL) and an aliquot of protein solution (2 μL). Crystals were obtained at 20 °C within 1 week. For cryo-protection, thus obtained crystals were soaked in the solution containing 40 % w/v Jeffamine ED-2001 and 0.1 M MES at pH 6.0 for overnight.

Data Collection of X-Ray Diffraction and Structure Determination: All the diffraction data were collected at the SPring-8 synchrotron facility (BL44XU, Harima, Hyogo, Japan). X-ray diffraction images were collected using an EIGER X 16M CCD detector (Dectris) equipped with a cryo-system at 100 K using a wavelength of 0.90000 Å. The data were processed and scaled with the XDS program package. The data collection and refinement statistics are summarized in Table S1. The crystal structures were solved by molecular replacement with the Phaser program[4] using the reported coordinate [apo-TM1459 (PDB code: 5WSD)] as a search model. The structure models were refined by the program phenix.refine,[5] manually rebuilding with the program Coot.[6] This procedure was iterated until the model did not further improve. Then, the structure model was further refined by SHELXL software (version 2017/1),[7] manually rebuilding with Coot. At this stage, anisotropic temperature factors were adapted to all the atoms except the hydrogen atoms and calculated with RIGU[8] and SIMU instructions. The restraint parameters of DFIX, DANG, and FLAT instructions for the MES was generated by using Grade Web Server (Global Phasing Ltd.). A subset of 5% of the reflections was separated to monitor the free *R* factor (R_{free}). In all the crystal structures, most of the residues were well defined in the final electron density, except for some disordered loops and amino acid residues in the flexible regions (Table S2). The distances and angles among the copper ions and their ligand atoms were completely unrestrained during structure refinement because the resolution and the data-to-parameter ratio were high enough. The bond lengths and angles of the metal-coordinating atoms to each metal including their estimated errors (for example, Cu–O (water) and Cu-imidazole Nε distances) are summarized in Table S3. In the structures, Ramachandran analysis with the Molprobity program[9] showed no outliners. The atomic coordinates of the final models and experimental structure factors have been deposited to the worldwide PDB and are accessible under the code described in Table S1. Secondary structures were assigned by the DSSP program[10] and all figures of protein structures were prepared using PyMOL (version 2.1, Schrödinger LLC).

Substrate Docking Simulation: The azachalcone was docked into cavity around Cu using AutoDock Vina[11] and PDBQT molecular structure files were made using AutoDock Tools.[12] The crystal structure coordinate of chain B of Cu-bound H52A/H58E mutant (PDB code: 8HJX) was used in the substrate-protein docking study. Water molecules were deleted, and hydrogens were added to the Cu-bound H52A/H58E structure before creating PDBQT files. Kollman all-atom charges for protein and Gasteiger−Hükel charges for the azachalcone were computed. The 2+ charge of the Cu ion was added to AutoDock Vina's atomic parameters. The side chains of

amino acids sitting around copper binding site (Lys24, Arg39, Phe41, Ile49, Trp56, Glu58, Phe94, Phe104, Cys106 (sulfinic acid),[1] and Ile108) were allowed to rotate during docking and all degrees of freedom were possible for the ligand. The search space was included in a 20 Å × 20 Å × 20 Å box to cover the complete binding site of the ligand around bound copper. At least 20 docking models for this mutant were generated and analyzed on the basis of scoring values of AutoDock's scoring function. PyMOL software was used to visualize the docking results. The pose with the pyridine moiety and ketone moiety pointing to Cu was selected.

Fluorescence experiments: Fluorescence quenching measurements were performed at 25 °C with a RF-5300PC (Shimadzu Corp.) as previously reported.[13] The excitation wavelength and spectral bandwidths were 265 nm and 5 nm, respectively. TM1459 mutants (final concentration, 1.2 μM) was titrated with a concentrated solution of $CuSO_4$ (3.2 mM). After each addition, the resulting solution was equilibrated for 5 min before the fluorescence measurement. The Cu^{2+} concentration was incrementally varied between 0-76 μM. Using emission intensity at 331 nm, fluorescence change was analyzed by curve fitting according to the one-ligand binding type equation previously reported.[13]

Catalytic Michael Addition of Dimethylmalonate: A vial (2 mL volume) was filled with 0.3 mL reaction solution, which is successively mixed with an aqueous solution of $CuSO_4$ (0.09 μmol, 30 μL), CH_3CN solution containing 2-azachalcone (3 μmol, 30 μL), apo-TM1459 (0.09 μmol) solution (20 mM phosphate buffer, pH 6.5) containing dimethylmalonate (final 150 mM). The mixture was stirred (600 rpm) in the closed vial at 30 °C for 6 hours. After the reaction, 4-methoxy-1-naphthol was added to the mixture as an internal standard. Then, the product was isolated by extraction with ethyl acetate. After drying (Na_2SO_4), the crude product was analyzed by HPLC equipped with a normal-phase chiral column [CHIRAL ART Amylose-SA, (5 μm, 4.6 × 250 mm, YMC Co., Ltd.)] via comparison with authentic standards to determine the yields, enantiomeric excess (*ee*) and diastereomeric ratio (*d.r.*). The yields were calculated from a calibration curve: a plot of mole ratio (moles of organic compound / moles of internal standard) versus area ratio (area of organic compound/area of standard).

Catalytic Michael Addition of Methyl acetoacetate: A vial (2 mL volume) was filled with 0.3 mL reaction solution, which is successively mixed with an aqueous solution of $CuSO_4$ (0.09 μmol, 30 μL), CH_3CN solution containing 2-azachalcone (3 μmol, 30 μL), apo-TM1459 (0.09 μmol) solution (20 mM phosphate buffer, pH 6.5) containing methyl acetoacetate (final 60 mM). The mixture was stirred (600 rpm) in the closed vial at 20 °C for 16 hours. After the reaction, 1-naphthol was added to the mixture as an internal standard. Then, the product was isolated by extraction with ethyl acetate. After drying (Na_2SO_4), the crude product was analyzed by HPLC equipped with a normal-phase chiral column [CHIRAL ART Amylose-SA (5 μm, 4.6 × 250 mm, YMC Co.,

Ltd.)] via comparison with authentic standards to determine the yields, enantiomeric excess (*ee*) and diastereomeric ratio (*d.r.*). The yields were calculated from a calibration curve: a plot of mole ratio (moles of organic compound / moles of internal standard) versus area ratio (area of organic compound/area of standard).

Michaelis-Menten Kinetics: Kinetic assays were also performed similarly to the catalytic assays, but 1, 2, 4, 8 or 16 equiv. of methyl acetoacetate to 2-azachalcone were added in reaction mixture. Additionally, assays were quenched upon the addition of acetonitrile at either 2 h, 3 h, or 4 h. The crude product was analyzed by HPLC equipped with a reverse-phase chiral column [ZORBAX Eclipse XDB-C8 (5 μm, 4.6 × 150 mm, Agilent Technologies, Inc.)] via comparison with authentic standards to determine the amount of product. The reaction velocity (v_{obs}) was calculated from the initial slope. Steady-state kinetic parameters (catalytic turnover number (k_{cat}) and Michaelis constant (K_M) were determined by nonlinear fitting of Michaelis-Menten plots.

Synthesis of (*E*)-3-phenyl-1-(pyridin-2-yl)prop-2-en-1-one (1): The substrate, 1,2-unsaturated ketones, 2-azachalcone **1**, were readily prepared from aldol condensation reaction according to modified reported procedures.[14] ^{1}H NMR (500 MHz, $CDCl_3$), δ = 8.76-8.75 (m, 1H), 8.31 (d, J = 16.0 Hz, 1H), 8.20 (dt, J = 8.0, 1.2 Hz, 1H), 7.95 (d, J = 16.0 Hz, 1H), 7.87 (td, J = 7.5, 1.7 Hz, 1H), 7.75-7.73 (m, 2H), 7.50 (ddd, J = 7.5, 4.6, 1.2 Hz, 1H), 7.44-7.42 (m, 3H) ppm. ^{13}C NMR (125 MHz, $CDCl_3$): δ =189.5, 154.2, 148.8, 144.8, 137.0, 135.1, 130.6, 128.9, 128.8, 126.9, 122.9, 120.8 ppm (Figure S8A). MS (+ESI): *m*/*z* calcd. for $C_{14}H_{12}NO$ $[M+H]^+$: 210.2, found 210.2; consistent with the ^{1}H and ^{13}C NMR, and mass spectroscopic data previously reported for this compound.[15–18]

Synthesis of Dimethyl 2-(3-oxo-1-phenyl-3-(pyridine-2-yl)propyl)malonate (2): Compound **2** for authentic standard (racemic product) was synthesized following procedure. A flask (300 mL volume) was filled with 100 mL reaction solution, which is successively mixed with an aqueous solution of $CuSO_4$ (3 μmol, 10 mL), CH_3CN solution containing 2-azachalcone **1** (100 μmol, 10 mL), 20 mM phosphate buffer, pH 6.5, containing dimethylmalonate (final 150 mM). The mixture was stirred at room temperature for 72 h, then the product was isolated by extraction with ethyl acetate. After drying (Na_2SO_4), purified by silica gel column chromatography (hexane/EtOAc, 70:30). Retention time on HPLC: t_R = 20.2 (–), 22.4 (+) min (CHIRAL ART Amylose-SA; hexane/iPrOH, 95:5; 1 mL/min), t_R = 9.9 [*R*-(–)], 10.7 [*S*-(+)] min (CHIRALPAK IA-3; hexane/iPrOH, 60:40; 1 mL/min); ^{1}H NMR (500 MHz, $CDCl_3$), δ = 8.65-8.64 (m, 1H), 7.91 (d, J = 7.5 Hz, 1H), 7.78-7.74 (m, 1H), 7.44-7.41 (m, 1H), 7.32-7.30 (m, 2H), 7.25-7.22 (m, 2H), 7.17-7.14 (m, 1H), 4.22 ((td, J = 9.7, 4.6 Hz, 1H), 3.93 (dd, J = 17.8, 9.2 Hz, 1H), 3.86 (d, J = 10.3 Hz, 1H), 3.72 (s, 3H), 3.61 (dd, J = 18.3, 4.6 Hz, 1H), 3.47 (s, 3H) ppm. ^{13}C NMR (125 MHz, $CDCl_3$): δ = 198.9, 168.6, 168.2, 153.2, 148.9, 140.8, 136.8, 128.4, 128.3, 127.1. 127.0, 121.8, 57.7, 52.6, 52.3, 41.7, 40.5 ppm (Figure S8B). MS (+ESI): *m*/*z* calcd. for $C_{19}H_{19}NO_5$ [M

+ H]$^+$: 342.1, found: 342.1; consistent with the ^{1}H and ^{13}C NMR, and mass spectroscopic data previously reported for this compound.[19] *N*-oxygenation of compound **2** to corresponding pyridine *N*-oxide adduct allowed us to determine the absolute stereochemistry of the stereogenic center according to the literature (vide infra).[17]

Synthesis of Dimethyl 2-(3-oxo-1-phenyl-3-(pyridine-*N*-oxide-2-yl)propyl)malonate (2'): Compound **2'** for authentic standard (racemic product) was synthesized according to reported procedures with some modification.[20] Compound **2** was solved in acetic acid and H_2O_2 (aq, 30 %) was added. The mixture was heated to 70 °C for 72 h, then the product was isolated by extraction with ethyl acetate. After drying (Na_2SO_4), purified by silica gel column chromatography (hexane/acetone, 50:50). Retention time on HPLC: t_R = 14.0 [*S*-(+)], 15.0 [*R*-(–)] min (CHIRALPAK IA-3; hexane/iPrOH, 60:40; 1 mL/min); ^{1}H NMR (500 MHz, $CDCl_3$), δ = 8.15-8.14 (m, 1H), 7.31-7.28 (m, 2H), 7.25-7.14 (m, 6H), 4.13-4.10 (m, 1H), 3.88 (dd, *J* = 17.2, 9.7 Hz, 1H), 3.79 (d, *J* = 10.3 Hz, 1H), 3.75 (s, 3H), 3.63 (dd, *J* = 17.2, 4.6 Hz, 1H), 3.46 (s, 3H) ppm. ^{13}C NMR (125 MHz, $CDCl_3$): δ = 195.2, 168.4, 168.0, 146.6, 140.4, 140.3, 128.4, 128.3, 127.8, 127.2, 126.8, 125.5, 57.5, 52.7, 52.4, 46.9, 41.0 ppm (Figure S8C). MS (+ESI): *m*/*z* calcd. for $C_{19}H_{19}NO_6$ [M+H]$^+$: 358.3, found: 358.0; consistent with the ^{1}H and ^{13}C NMR, and mass spectroscopic data previously reported for this compound.[20]

***N*-oxygenation of enzymatic product (compound 2):** A flask (100 mL volume) was filled with 9 mL reaction solution (catalytic Michael addition of dimethylmalonate), which is successively mixed with an aqueous solution of $CuSO_4$ (2.7 μmol, 900 μL), CH_3CN solution containing 2-azachalcone **1** (90 μmol, 900 μL), apo-TM1459 H52A variant (2.7 μmol) solution (20 mM phosphate buffer, pH 6.5) containing dimethylmalonate (final 150 mM). The mixture was stirred at room temperature for 24 h, then the product was isolated by extraction with ethyl acetate. After drying (Na_2SO_4), purified by silica gel column chromatography (hexane/EtOAc, 70:30). The products thus obtained was *N*-oxygenated upon the addition of hydrogen peroxide following the reported procedures.[20] Then, the resultant mixture was extracted with ethyl acetate and the organic layer was analyzed by HPLC equipped with a normal-phase chiral column (CHIRALPAK IA-3). The two peaks (minor: t_R = 13.6 [*S*-(+)], major: t_R = 14.4 [*R*-(–)] min, Figure S3B) additionally appeared, which could correspond to *N*-oxygenated compound **2'**, while *N*-deoxygenated compound **2** exhibited the two peaks (major: t_R = 9.9 (–) min, minor: t_R =10.7 (+) min, Figure S3B). Namely, the former peak and the latter peak can be assigned to *R*- and *S*-form, respectively, indicating that H52A prefers *R*-isomer. Since the structure of dimethylmalonate is similar to that of methyl acetoacetate, the absolute stereochemistry could be assigned on the assumption of a common stereochemical pathway. These results indicate the preference of the methyl acetoacetate to attack from the *Si*-face of the double bond of the azachalcone **1** with H52A variant.

Synthesis of methyl 2-acetyl-5-oxo-3-phenyl-5-(pyridin-2-yl)pentanoate (3): Compound **3** for authentic standard (racemic product) was synthesized as the following procedure. A flask (300 mL volume) was filled with 80 mL reaction solution, which is successively mixed with an aqueous solution of $CuSO_4$ (35 μmol, 60 mL) and CH_3CN solution containing 2-azachalcone **1** (1.4 mmol, 14 mL) and methyl acetoacetate (final 700 mM). Then the product was isolated by extraction with ethyl acetate. After drying (Na_2SO_4), purified by silica gel column chromatography (hexane/EtOAc, 80:20), and obtained almost pure product in 25 %. Retention time on HPLC: t_R = 17.6 (+)-*anti*, 18.5 (–)-*anti*, 21.2 (–)-*syn*, and 24.1 (+)-*syn* (CHIRAL ART Amylose-SA; hexane/iPrOH, 98:2; 1 mL/min, Figure S4); HRMS (+ESI): *m/z* calcd. for $C_{19}H_{19}NO_4$ $[M+Na]^+$: 348.1211, found: 348.1213. Each diastereomer was isolated by chiral stationary column on HPLC. ***Anti*-isomer:** ^{1}H NMR (500 MHz, $CDCl_3$), δ =8.64 (d, J = 4.6 Hz, 1H), 7.90 (dt, J = 8.0, 1.2 Hz, 1H), 7.77 (td, J = 7.7, 1.7 Hz, 1H), 7.43 (ddd, J = 7.5, 5.2, 1.2 Hz, 1H), 7.29 (d, J = 6.9 Hz, 2H), 7.23 (t, J = 7.7 Hz, 2H), 7.15 (t, J = 7.5 Hz, 1H), 4.25-4.20(m, 1H), 4.00 (d, J = 10.9 Hz, 1H), 3.79 (dd, J = 17.5, 9.7 Hz, 1H), 3.46 (dd, J = 17.6, 4.6 Hz, 1H), 3.44 (s, 3H), 2.31 (s, 3H) ppm. ^{13}C NMR (125 MHz, $CDCl_3$): δ = 202.1, 199.0, 168.5, 153.0, 148.8, 140.9, 136.9, 128.4, 128.2, 127.2, 127.0, 121.2, 66.0, 52.3, 41.8, 40.1, 29.5 ppm (Figure S8D). ***Syn*-isomer:** ^{1}H NMR (500 MHz, $CDCl_3$), δ =8.65-8.63 (m, 1H), 7.91 (d, J = 8.0 Hz, 1H), 7.77 (td, J = 8.0, 1.7 Hz, 1H), 7.43 (ddd, J = 7.5, 4.6, 1.2 Hz, 1H), 7.30 (d, J = 8.0 Hz, 2H), 7.24 (t, J = 7.7 Hz, 2H), 7.15 (t, J = 7.2 Hz, 2H), 4.25-4.20 (m, 1H), 4.03 (d, J = 10.9 Hz, 1H), 3.90 (dd, J = 18.0, 9.5 Hz, 1H), 3.72 (s, 3H), 3.53 (dd, J = 17.8, 4.0 Hz ,1H), 1.96 (s, 3H) ppm. ^{13}C NMR (125 MHz, $CDCl_3$): δ = 202.2, 198.8, 168.9, 153.1, 148.8, 140.7, 136.8, 128.6, 128.3, 127.2, 127.1, 121.8, 65.0, 52.6, 42.1, 40.5, 30.1 ppm (Figure S8E). The relative configuration of diastereomers (*anti* or *syn*-isomer) was determined by analogy with similar compound, in which the diastereoisomer with the singlet CH_3CO at lower field and the CH_3 in methoxy group at higher field was assigned as anti-isomer according to the literature.[21,22]

Supporting References

(1) Fujieda, N.; Nakano, T.; Taniguchi, Y.; Ichihashi, H.; Sugimoto, H.; Morimoto, Y.; Nishikawa, Y.; Kurisu, G.; Itoh, S. A Well-Defined Osmium–Cupin Complex: Hyperstable Artificial Osmium Peroxygenase. *J. Am. Chem. Soc.* **2017**, *139* (14), 5149–5155. https://doi.org/10.1021/jacs.7b00675.

(2) Fujieda, N.; Ichihashi, H.; Yuasa, M.; Nishikawa, Y.; Kurisu, G.; Itoh, S. Cupin Variants as a Macromolecular Ligand Library for Stereoselective Michael Addition of Nitroalkanes. *Angew. Chemie Int. Ed.* **2020**, *59* (20), 7717–7720. https://doi.org/10.1002/anie.202000129.

(3) Gill, S. C.; von Hippel, P. H. Calculation of Protein Extinction Coefficients from Amino Acid Sequence Data. *Anal. Biochem.* **1989**, *182* (2), 319–326. https://doi.org/10.1016/0003-2697(89)90602-7.

(4) McCoy, A. J.; Grosse-Kunstleve, R. W.; Adams, P. D.; Winn, M. D.; Storoni, L. C.; Read, R. J. Phaser Crystallographic Software. *J. Appl. Crystallogr.* **2007**, *40* (4), 658–674. https://doi.org/10.1107/S0021889807021206.

(5) Adams, P. D.; Afonine, P. V.; Bunkóczi, G.; Chen, V. B.; Davis, I. W.; Echols, N.; Headd, J. J.; Hung, L.-W.; Kapral, G. J.; Grosse-Kunstleve, R. W.; et al. PHENIX : A Comprehensive Python-Based System for Macromolecular Structure Solution. *Acta Crystallogr. Sect. D* **2010**, *66* (2), 213–221. https://doi.org/10.1107/S0907444909052925.

(6) Emsley, P.; Cowtan, K. Coot: Model-Building Tools for Molecular Graphics. *Acta Crystallogr. Sect. D* **2004**, *60* (12), 2126–2132. https://doi.org/10.1107/S0907444904019158.

(7) Sheldrick, G. M. A Short History of SHELX. *Acta Crystallographica Section A: Foundations of Crystallography*. International Union of Crystallography 2008, pp 112–122. https://doi.org/10.1107/S0108767307043930.

(8) Thorn, A.; Dittrich, B.; Sheldrick, G. M. Enhanced Rigid-Bond Restraints. *Acta Crystallogr. Sect. A* **2012**, *68* (4), 448–451. https://doi.org/10.1107/S0108767312014535.

(9) Chen, V. B.; Arendall, W. B.; Headd, J. J.; Keedy, D. A.; Immormino, R. M.; Kapral, G. J.; Murray, L. W.; Richardson, J. S.; Richardson, D. C. MolProbity : All-Atom Structure Validation for Macromolecular Crystallography. *Acta Crystallogr. Sect. D* **2010**, *66* (1), 12–21. https://doi.org/10.1107/S0907444909042073.

(10) Kabsch, W.; Sander, C. Dictionary of Protein Secondary Structure: Pattern Recognition of Hydrogen-Bonded and Geometrical Features. *Biopolymers* **1983**, *22* (12), 2577–2637. https://doi.org/10.1002/bip.360221211.

(11) Trott, O.; Olson, A. J. AutoDock Vina: Improving the Speed and Accuracy of Docking with a New Scoring Function, Efficient Optimization, and Multithreading. *J. Comput. Chem.* **2009**, *31* (2), 455−461. https://doi.org/10.1002/jcc.21334.

(12) Morris, G. M.; Huey, R.; Lindstrom, W.; Sanner, M. F.; Belew, R. K.; Goodsell, D. S.; Olson, A. J. AutoDock4 and AutoDockTools4: Automated Docking with Selective Receptor Flexibility. *J. Comput.*

Chem. **2009**, *30* (16), 2785–2791. https://doi.org/10.1002/jcc.21256.

(13) Brisson, L.; El Bakkali-Taheri, N.; Giorgi, M.; Fadel, A.; Kaizer, J.; Réglier, M.; Tron, T.; Ajandouz, E. H.; Simaan, A. J. 1-Aminocyclopropane-1-Carboxylic Acid Oxidase: Insight into Cofactor Binding from Experimental and Theoretical Studies. *J. Biol. Inorg. Chem.* **2012**, *17* (6), 939–949. https://doi.org/10.1007/s00775-012-0910-3.

(14) Otto, S.; Bertoncin, F.; Engberts, J. B. F. N. Lewis Acid Catalysis of a Diels-Alder Reaction in Water. *J. Am. Chem. Soc.* **1996**, *118* (33), 7702–7707. https://doi.org/10.1021/ja960318k.

(15) Gase, R. A.; Pandit, U. K. Reduced Nicotinamide Adenine Dinucleotide (NADH) Models. 14.1 Metal Ion Catalysis of the Reduction of Aβ-Unsaturated Ketones by 1,4-Dihydropyridines. A Model of Δ4-3-Ketosteroid Reductases. *J. Am. Chem. Soc.* **1979**, *101* (23), 7059–7064. https://doi.org/10.1021/ja00517a047.

(16) Ciupa, A.; Mahon, M. F.; De Bank, P. A.; Caggiano, L. Simple Pyrazoline and Pyrazole "Turn on" Fluorescent Sensors Selective for Cd^{2+} and Zn^{2+} in MeCN. *Org. Biomol. Chem.* **2012**, *10* (44), 8753–8757. https://doi.org/10.1039/c2ob26608c.

(17) Punt, P. M.; Langenberg, M. D.; Altan, O.; Clever, G. H. Modular Design of G-Quadruplex MetalloDNAzymes for Catalytic C–C Bond Formations with Switchable Enantioselectivity. *J. Am. Chem. Soc.* **2021**, *143* (9), 3555–3561. https://doi.org/10.1021/jacs.0c13251.

(18) Balázs, L. B.; Tay, W. S.; Li, Y.; Pullarkat, S. A.; Leung, P.-H. Synthesis of Stereoprojecting, Chiral N-C(Sp^3)-E Type Pincer Complexes. *Organometallics* **2018**, *37* (14), 2272–2285. https://doi.org/10.1021/acs.organomet.8b00262.

(19) Blay, G.; Incerti, C.; Muñoz, M. C.; Pedro, J. R. Enantioselective La^{III}-PyBOX-Catalyzed Nitro-Michael Addition to (*E*)-2-Azachalcones. *European J. Org. Chem.* **2013**, *2013* (9), 1696–1705. https://doi.org/10.1002/ejoc.201201579.

(20) Ray, S. K.; Singh, P. K.; Singh, V. K. Enantioselective Michael Addition of Malonates to 2-Enoylpyridine *N*-Oxides Catalyzed by Chiral Bisoxazoline–Zn(II) Complex. *Org. Lett.* **2011**, *13* (21), 5812–5815. https://doi.org/10.1021/ol202405v.

(21) Christoffers, J. Novel Chemoselective and Diastereoselective Iron(III)-Catalysed Michael Reactions of 1,3-Dicarbonyl Compounds and Enones. *J. Chem. Soc. - Perkin Trans. 1* **1997**, No. 21, 3141–3149. https://doi.org/10.1039/a704873d.

(22) Zhang, Z.; Dong, Y.-W.; Wang, G.-W.; Komatsu, K. Mechanochemical Michael Reactions of Chalcones and Azachalcones with Ethyl Acetoacetate Catalyzed by K_2CO_3 under Solvent-Free Conditions. *Chem. Lett.* **2004**, *33* (2), 168–169. https://doi.org/10.1246/cl.2004.168.

Table S1. Data collection and refinement statistics.[a]

	H52A/H58E mutant (PDB code: 8HJX)	H52A/H58E/F104W mutant (PDB code: 8HJY)	H52A/H58Q mutant (PDB code: 8HJZ)
Dataset			
X-ray source	Spring-8 BL44XU	Spring-8 BL44XU	Spring-8 BL44XU
Space group	$P2_12_12_1$	$P2_12_12_1$	$P2_12_12_1$
Unit cell	a = 50.706 Å, b = 57.763 Å, c = 75.317 Å, $\alpha = \beta = \gamma = 90^\circ$	a = 50.697 Å, b = 57.716 Å, c = 75.825 Å, $\alpha = \beta = \gamma = 90^\circ$	a = 51.103 Å, b = 57.779 Å, c = 74.977 Å, $\alpha = \beta = \gamma = 90^\circ$
Wavelength	0.90000 Å	0.90000 Å	0.90000 Å
Resolution	50 to 1.15 Å	50 to 1.18 Å	50 to 1.22 Å
No. reflection (total/unique)	517421 / 151673	487019 / 141051	434064 / 127123
Redundancy[b]	3.41 (3.38)	3.45 (3.41)	3.41 (3.13)
Completeness[b]	99.0% (99.2%)	99.0% (98.4%)	98.8% (94.5%)
R_{merge}[b]	5.4% (58.5%)	7.2% (83.1%)	6.6% (59.6%)
I/σ[b]	11.2 (2.13)	26.2 (2.9)	10.2 (2.10)
CC(1/2)	99.7 (72.6)	99.5 (70.6)	99.7 (71.8)
Refinement			
R_{work}/R_{free}	0.1456/0.1838	0.1530/0.1925	0.1501/0.1883
No. of protein/solvent atoms[c]	1941/255	1903/217	1921/207
No. of metal ion atoms	3	3	3
B-factors of protein/solvent	19.0/37.5	20.1/38.0	17.5/35.9
B-factors of metal ions	21.0	24.7	17.5
r.m.s.d. bond/angle	0.012/2.10	0.011/2.07	0.011/1.97
Ramchandran favored/allowed[d]	98.7%/1.3%	99.1%/0.9%	98.7%/1.3%

[a]A single crystal was used for all of structures. [b]Values in parentheses are for highest-resolution shell. [c]Hydrogen atoms not included. [d]Values are calculated by Molprobity.

Table S2. Missing residues and atoms.

H52A/H58E (PDB code: 8HJX)
Missing residues
Chain B, Gly(-3)–Ser(-1)
Missing atoms
Chain A, Gln12 (Cγ, Cδ, Oε1, Nε2), Asp17 (Cγ, Oδ1, Oδ2), Arg20 (Cγ, Cδ, Nε, Cζ, Nη1, Nη2), Lys66 (Cδ, Cε, Nζ), Gln73 (Cδ, Oε1, Nε2),
Chain A, Glu79 (Cδ, Oε1, Oε2)
Chain B, Lys4 (Cε, Nζ), Asp17 (Cβ, Cγ, Oδ1, Oδ2), Lys18 (Cγ, Cδ, Cε, Nζ), Lys31 (Cδ, Cε, Nζ), Lys66 (Cγ, Cδ, Cε, Nζ),
Chain B, Gln73 (Cγ, Cδ, Oε1, Nε2), Glu79 (Oε1, Oε2)
H52A/H58E/F104W (PDB code: 8HJY)
Missing residues
Chain B, Gly(-3)–Ser(-1)
Missing atoms
Chain A, Gln12 (Cδ, Oε1, Nε2), Asp17 (Cγ, Oδ1, Oδ2), Lys66 (Cγ, Cδ, Cε, Nζ), Gln73 (Cγ, Cδ, Oε1, Nε2)
Chain B, Asp17 (Cγ, Oδ1, Oδ2), Lys18 (Cγ, Cδ, Cε, Nζ), Arg20 (Cγ, Cδ, Nε, Cζ, Nη1, Nη2), Lys31 (Cγ, Cδ, Cε, Nζ), Asp50 (Cγ, Oδ1, Oδ2),
Chain B, Lys66 (Cγ, Cδ, Cε, Nζ), Gln73 (Cγ, Cδ, Oε1, Nε2), Glu79 (Oε1, Oε2), Glu103 (Cδ, Oε1, Oε2), Lys110 (Nζ)
H52A/H58Q (PDB code: 8HJZ)
Missing residues
Chain B, Gly(-3)–Pro(-2)
Missing atoms
Chain A, Gln12 (Cδ, Oε1, Nε2), Arg20 (Cδ, Nε, Cζ, Nη1, Nη2), Lys66 (Cε, Nζ), Gln73 (Cγ, Cδ, Oε1, Nε2)
Chain B, Asp17 (Cβ, Cγ, Oδ1, Oδ2), Lys18 (Cγ, Cδ, Cε, Nζ), Lys31 (Cγ, Cδ, Cε, Nζ), Lys66 (Cγ, Cδ, Cε, Nζ), Glu79 (Cδ, Oε1, Oε2)

Table S3. Interatomic distances and bond angles in the crystal structures (Cu ion and coordinating atoms)

H52A/H58E (PDB code: 8HJX)					
Chain A					
Bond Lengths[a]					
	His54(Nε)	Glu58(Oε1)	His92(Nε)	O1	O2
Cu	2.06 (0.02)	2.27 (0.03)	2.00 (0.02)	2.19 (0.03)	1.97 (0.04)
Angles[a]					
Cu	His54(Nε)	Glu58(Oε1)	His92(Nε)	O1	O2
His54(Nε)					
Glu58(Oε1)	91.0 (1.0)				
His92(Nε)	99.7 (0.7)	90.4 (1.3)			
O1	161.7 (1.3)	98.5 (1.7)	95.8 (0.9)		
O2	86.7 (1.4)	104.0 (2.4)	164.2 (1.9)	75.8 (1.6)	
Chain B					
Bond Lengths[a]					
	His54(Nε)	Glu58(Oε1)	His92(Nε)	O1	O2
Cu(major)	2.13 (0.04)	2.20 (0.03)	2.01 (0.02)	2.06 (0.03)	1.99 (0.03)
Cu(minor)	1.93 (0.06)	2.73 (0.04)	2.02 (0.02)	1.98 (0.03)	1.93 (0.03)
Angles[a]					
Cu(major)	His54(Nε)	Glu58(Oε1)	His92(Nε)	O1	O2
His54(Nε)					
Glu58(Oε1)	88.8 (1.4)				
His92(Nε)	98.3 (1.0)	94.7 (1.3)			
O1	168.2 (1.5)	92.9 (1.5)	93.2 (1.1)		
O2	94.4 (1.5)	103.9 (1.9)	157.7 (1.7)	73.9 (1.6)	
Angles[a]					
Cu(minor)	His54(Nε)	Glu58(Oε1)	His92(Nε)	O1	O2
His54(Nε)					
Glu58(Oε1)	108.0 (2.1)				
His92(Nε)	105.0 (1.7)	80.0 (1.2)			
O1	159.0 (2.1)	80.2 (1.5)	95.4 (1.3)		
O2	84.0 (1.9)	88.4 (1.9)	167.1 (1.8)	76.9 (1.6)	

[a]Distances and angles are given in Å and degrees (°), estimated errors are given in parentheses.

H52A/H58E/F104W (PDB code: 8HJY)				
Chain A				
Bond Lengths[a]				
	His54(Nε)	Glu58(Oε1)	His92(Nε)	O1
Cu	2.07 (0.02)	2.54 (0.05)	2.05 (0.02)	2.42 (0.06)
Angles[a]				
Cu	His54(Nε)	Glu58(Oε1)	His92(Nε)	O1
His54(Nε)				
Glu58(Oε1)	104.1 (1.3)			
His92(Nε)	102.1 (0.8)	93.7 (1.7)		
O1	160.9 (2.2)	84.5 (2.7)	94.2 (1.3)	
Chain B				
Bond Lengths[a]				
	His54(Nε)	Glu58(Oε1)	His92(Nε)	O1
Cu(major)	2.31 (0.05)	1.85 (0.04)	1.93 (0.03)	1.97 (0.04)
Cu(minor)	1.90 (0.08)	2.66 (0.04)	2.12 (0.03)	1.95 (0.04)
Angles[a]				
Cu(major)	His54(Nε)	Glu58(Oε1)	His92(Nε)	O1
His54(Nε)				
Glu58(Oε1)	92.5 (1.8)			
His92(Nε)	99.6 (1.3)	102.8 (2.2)		
O1	152.5 (2.1)	103.8 (2.0)	98.3 (1.6)	
Cu(minor)	His54(Nε)	Glu58(Oε1)	His92(Nε)	O1
His54(Nε)				
Glu58(Oε1)	112.5 (2.7)			
His92(Nε)	109.5 (2.4)	75.6 (1.5)		
O1	156.4 (2.9)	79.8 (1.8)	92.9 (1.6)	

[a]Distances and angles are given in Å and degrees (°), estimated errors are given in parentheses.

H52A/H58Q (PDB code: 8HJZ)					
Chain A					
Bond Lengths[a]					
	His54(Nε)	Gln58(Oε1)	His92(Nε)	O1	
Cu	2.01 (0.02)	2.11 (0.03)	2.00 (0.02)	2.16 (0.03)	
Angles[a]					
Cu	His54(Nε)	Gln58(Oε1)	His92(Nε)	O1	
His54(Nε)					
Gln58(Oε1)	89.3 (1.1)				
His92(Nε)	101.4 (0.8)	100.2 (1.3)			
O1	155.1 (1.4)	100.6 (1.4)	99.2 (1.3)		
Chain B					
Bond Lengths[a]					
	His54(Nε)	Gln58(Oε1)	His92(Nε)	O1	O2
Cu(major)	2.07 (0.04)	2.49 (0.11)	1.91 (0.02)	3.23 (0.05)	2.31 (0.03)
Cu(minor)	2.00 (0.07)	3.13 (0.06)	2.23 (0.03)	2.01 (0.05)	1.73 (0.04)
Angles[a]					
Cu(major)	His54(Nε)	Gln58(Oε1)	His92(Nε)	O1	O2
His54(Nε)					
Gln58(Oε1)	90.4 (2.9)				
His92(Nε)	103.5 (1.3)	86.9 (3.2)			
O1	113.1 (1.9)	156.2 (2.8)	91.4 (1.4)		
O2	153.7 (2.0)	112.9 (2.9)	90.3 (1.5)	43.3 (1.8)	
Cu(minor)	His54(Nε)	Gln58(Oε1)	His92(Nε)	O1	O2
His54(Nε)					
Gln58(Oε1)	82.0 (2.6)				
His92(Nε)	98.8 (1.7)	82.0 (1.9)			
O1	106.8 (2.8)	146.1 (2.6)	127.0 (1.8)		
O2	159.2 (2.3)	88.1 (3.0)	97.9 (1.9)	72.2 (2.5)	

[a]Distances and angles are given in Å and degrees (°), estimated errors are given in parentheses.

Table S4. Oligonucleotides used for site-directed mutagenesis of TM1459.[a]

No.	Sequence (5'-3')	Length	Use
1	TGGGAACATGAAATTTTCGTGCTGAAAGGCAAAC	34	Forward primer for H52A/H54E, H52E/H54A, H52E/H92A
2	CGGTTCGCTTGCGCGATCAATCAGACCACCCGGTT	35	Reverse primer for H52A/H54E
3	TGGGAAGAAGAAATTTTCGTGCTGAAAGGCAAAC	34	Forward primer for H52A/H58E, H54A/H58E
4	CGGATGGCTTGCGCGATCAATCAGACCACCCGGTT	35	Reverse primer for H52A/H58E
5	CGGTGCGCTTTCGCGATCAATCAGACCACCCGGTT	35	Reverse primer for H52E/H54A
6	CGGTGCGCTATGGCGATCAATCAGACCACCCGGTT	35	Reverse primer for H54A/H58E
7	TGGGAAGCAGAAATTTTCGTGCTGAAAGGCAAAC	34	Forward primer for H52E/H58A, H54E/H58A
8	CGGATGGCTTTCGCGATCAATCAGACCACCCGGTT	35	Reverse primer for H52E/H58A, H52E/H92A
9	CGGTTCGCTATGGCGATCAATCAGACCACCCGGTT	35	Reverse primer for H54E/H58A
10	TGGGAACAGGAAATTTTCGTGCTGAAAGGCAAAC	34	Forward primer for H52A/H58Q
11	CGGATGGCTTGCGCGATCAATCAGACCACCCGGTT	35	Reverse primer for H52A/H58Q
12	GATAAACTGCGTGGTGTTCGTAAACGTGTGCTG	33	Forward primer for H52A/H58E/V19L
13	ACCACGCAGTTTATCGGTTGAAATTTTCTGCGGTG	35	Reverse primer for H52A/H58E/V19L
14	ACGGTGGAACCGGGTGGTCTGATTG	25	Forward primer for H52A/H58E/F41W
15	CCACAGGCGCATCACAAAGTTCGGTGCATC	30	Reverse primer for H52A/H58E/F41W
16	GATCGCGCAAGCCATCCGTGGGAA	24	Forward primer for H52A/H58E/I49Q
17	TTGCAGACCACCCGGTTCCACCGTAAACAG	30	Reverse primer for H52A/H58E/I49Q
18	CTGTGCCTGATTCCGAAAGAAGGCGGAG	28	Forward primer for H52A/H58E/F104W
19	CCATTCCACTTCGCTATCGGTATCGTTGC	29	Reverse primer for H52A/H58E/F104W

[a] The mutagenic nucleotides are underlined.

Table S5. Screening of amount of dimethylmalonate with the H52A mutant in the Michael addition.[a,b]

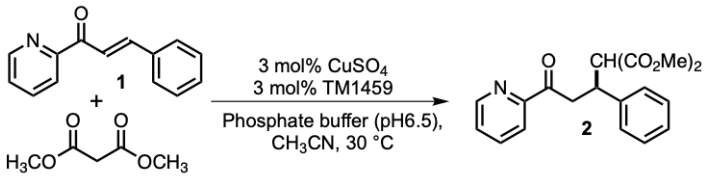

Entry	Catalyst	Dimethylmalonate (equiv.)	Yield (%)[c]	*ee* (%)[d]
1	H52A	3	37	88 (–)-(*R*)
2		5	41	88 (–)-(*R*)
3		15	48	86 (–)-(*R*)
4		30	44	86 (–)-(*R*)
5		88	35	84 (–)-(*R*)

[a]Reaction conditions: TM1459 (0.3 mM), Cu(II) sulfate (0.3 mM), **1** (10 mM), dimethylmalonate (30-880 mM), potassium phosphate buffer (pH 6.5)/CH_3CN (9:1), 30 °C, 6 h. [b]Yields and enantiomeric excesses (*ee*) were determined by chiral HPLC analysis. [c]Yields were calculated based on the total amount of stereoisomers [d](+) or (–) was determined by polarimeter on HPLC.

Table S6. Screening of reaction time with the H52A mutant in the Michael addition.[a,b]

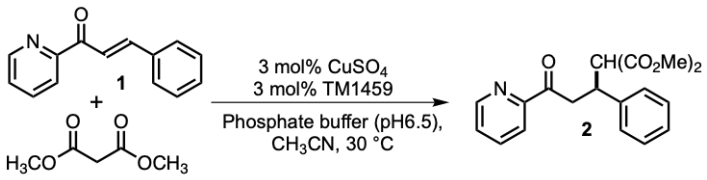

Entry	Catalyst	Time (h)	Yield (%)[c]	TON	*ee* (%)[d]
1	H52A	2	25	8	86 (*R*)
2		4	45	15	86 (*R*)
3		6	48	16	86 (*R*)
4		20	59	20	90 (*R*)
5		48	56	18	92 (*R*)

[a]Reaction conditions: TM1459 (0.3 mM), Cu(II) sulfate (0.3 mM), **1** (10 mM), dimethylmalonate (150 mM), potassium phosphate buffer (pH 6.5)/CH_3CN (9:1), 30 °C. [b]Yields and enantiomeric excesses (*ee*) were determined by chiral HPLC analysis. [c]Yields were calculated based on the total amount of (*S*) and (*R*). [d](+) or (-) was determined by polarimeter on HPLC.

Table S7. Addition of dimethylmalonate to azachalcones catalyzed by Cu-TM1459 and its mutants.[a, b]

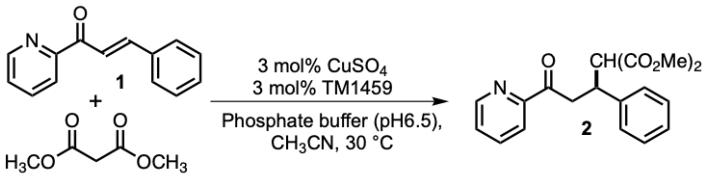

Entry	TM1459 Variant	Yield (%)[b,c]	*ee* (%)[d]
1	-	13	0
2	WT	0	n.d.
3	H52A	48	86(–)-(*R*)
4	H54A	11	1(+)-(*S*)
5	H58A	3	35(–)-(*R*)
6	H92A	17	58(+)-(*S*)

[a]Reaction conditions: TM1459 (0.3 mM), $CuSO_4$ (0.3 mM), **1** (10 mM), dimethylmalonate (150 mM), Potassium phosphate buffer (pH 6.5)/CH_3CN (9:1), 30 °C, 6 h. [b]Yields and enantiomeric excesses (*ee*) were determined by chiral HPLC analysis. [c]Yields were calculated based on the total amount of stereoisomers [d](+) or (–) was determined by polarimeter on HPLC.

Table S8. Screening of reaction time and catalyst amount with the H52A mutant in the Michael addition.[a,b]

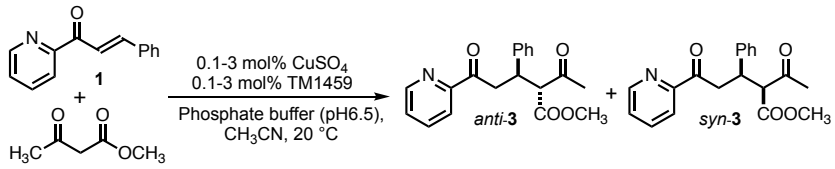

Entry	Catalyst	Time (h)	$CuSO_4$ (mol%)	TM1459 (mol%)	TON	Yield (%)[c]
1	H52A	2	3	3	17	53
2		4	3	3	21	65
3		6	3	3	23	70
4		16	3	3	27	82
5		24	3	3	33	99
6		16	1	1	88	88
7		16	0.5	0.5	109	55
8		16	0.1	0.1	n.d.	n.d.

[a]Reaction conditions: TM1459 (0.3 mM), CuSO4 (0.3 mM), 1 (10 mM), methyl acetoacetate (60 mM), potassium phosphate buffer (pH 6.5)/CH3CN (9:1), 20 °C, 16 h. [b]Yields were determined by chiral HPLC analysis. [c]Yields were calculated based on the total amount of stereoisomers.

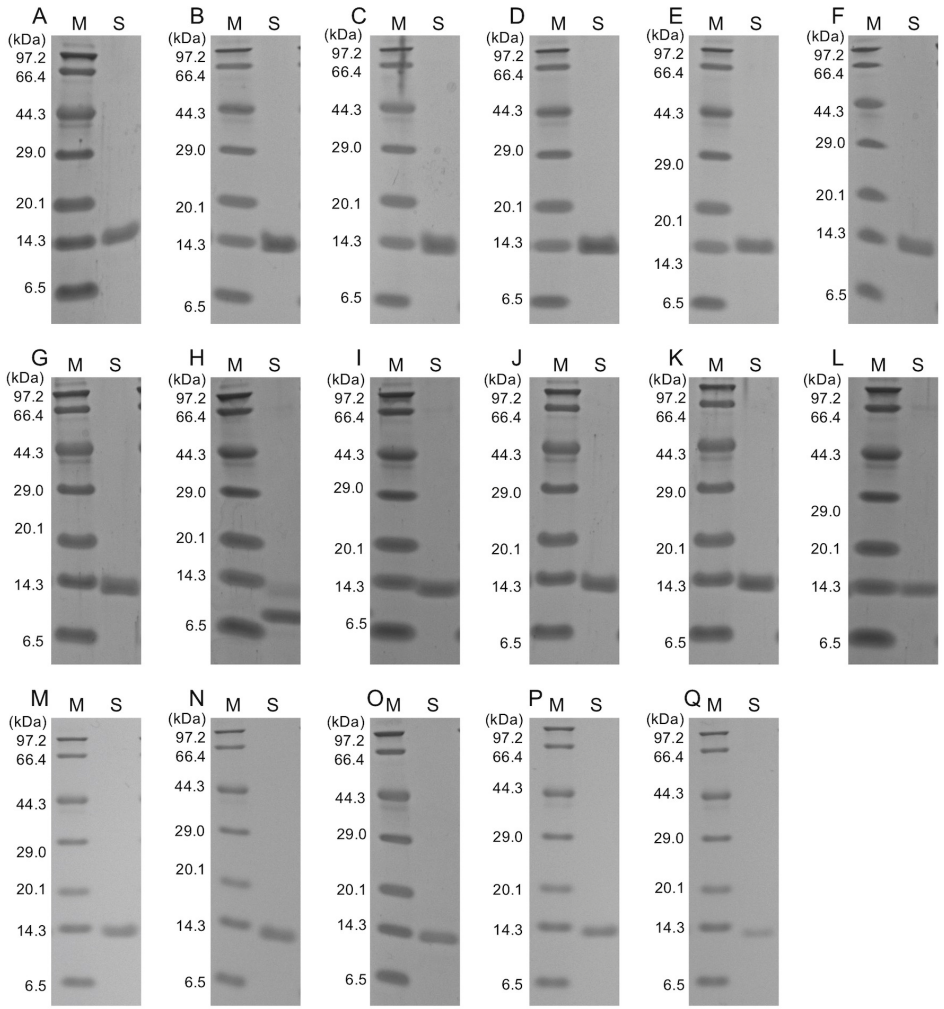

Figure S1. SDS-PAGE (Bis-tris 10 % acrylamide gel) analysis of the apo-TM1459 isoforms used in this study. (A) WT; (B) H52A; (C) H54A; (D) H58A; (E) H92A; (F) H52A/H54E; (G) H52A/H58E; (H) H52E/H54A; (I) H54A/H58E; (J) H52E/H58A; (K) H54E/H58A; (L) H52E/H92A (M) H52A/H58Q; (N) H52A/H58E/V19L; (O) H52A/H58E/F41W; (P) H52A/H58E/I49Q; (Q) H52A/H58E/F104W.

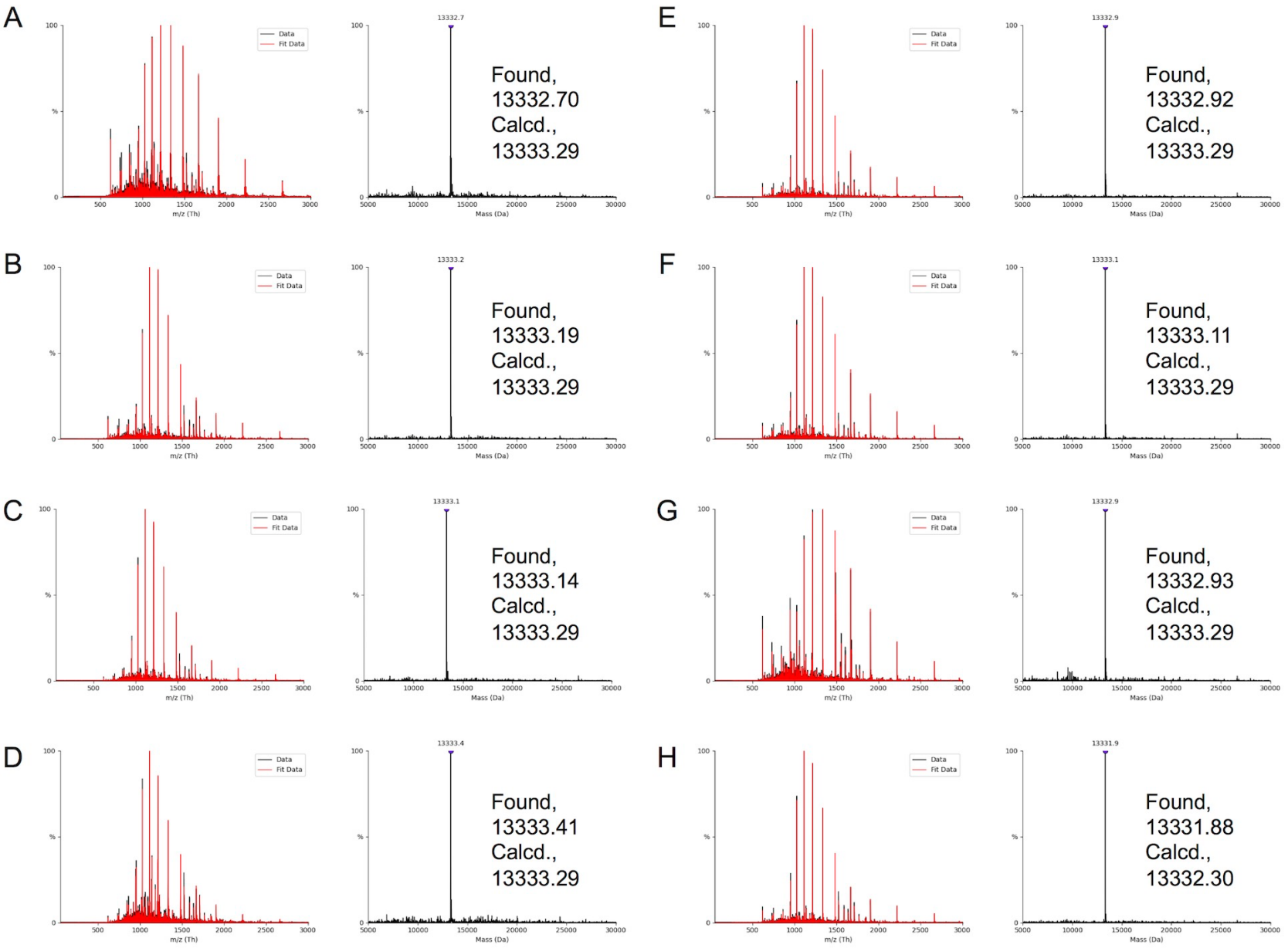
A
Data
Fit Data
m/z (Th)
13332.7
Mass (Da)
Found,
13332.70
Calcd.,
13333.29
B
13333.2
Found,
13333.19
Calcd.,
13333.29
C
13333.1
Found,
13333.14
Calcd.,
13333.29
D
13333.4
Found,
13333.41
Calcd.,
13333.29
E
13332.9
Found,
13332.92
Calcd.,
13333.29
F
13333.1
Found,
13333.11
Calcd.,
13333.29
G
13332.9
Found,
13332.93
Calcd.,
13333.29
H
13331.9
Found,
13331.88
Calcd.,
13332.30

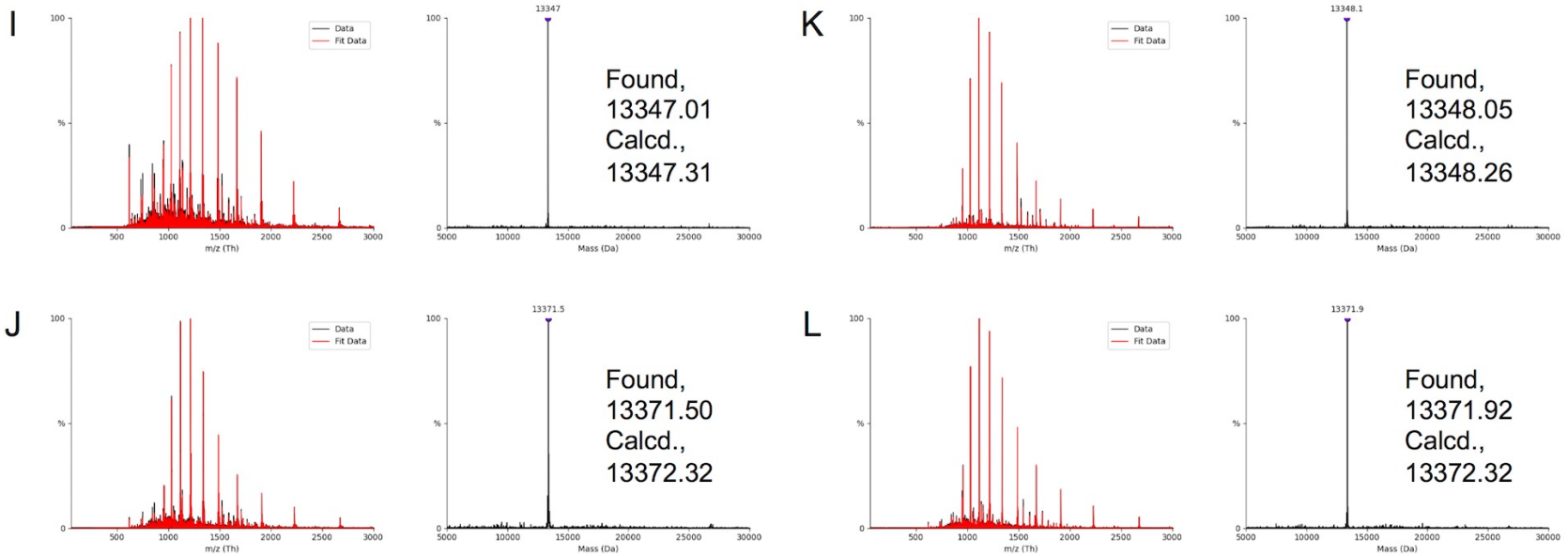

Figure S2. Non-deconvoluted (left) and deconvoluted (right) ESI-TOF/MS spectra of multiply-charged ions of the apo-TM1459 isoforms used in this study. (A) H52A/H54E; (B) H52A/H58E; (C) H52E/H54A; (D) H54A/H58E; (E) H52E/H58A; (F) H54E/H58A; (G) H52E/H92A (H) H52A/H58Q; (I) H52A/H58E/V19L; (J) H52A/H58E/F41W; (K) H52A/H58E/I49Q; (L) H52A/H58E/F104W.

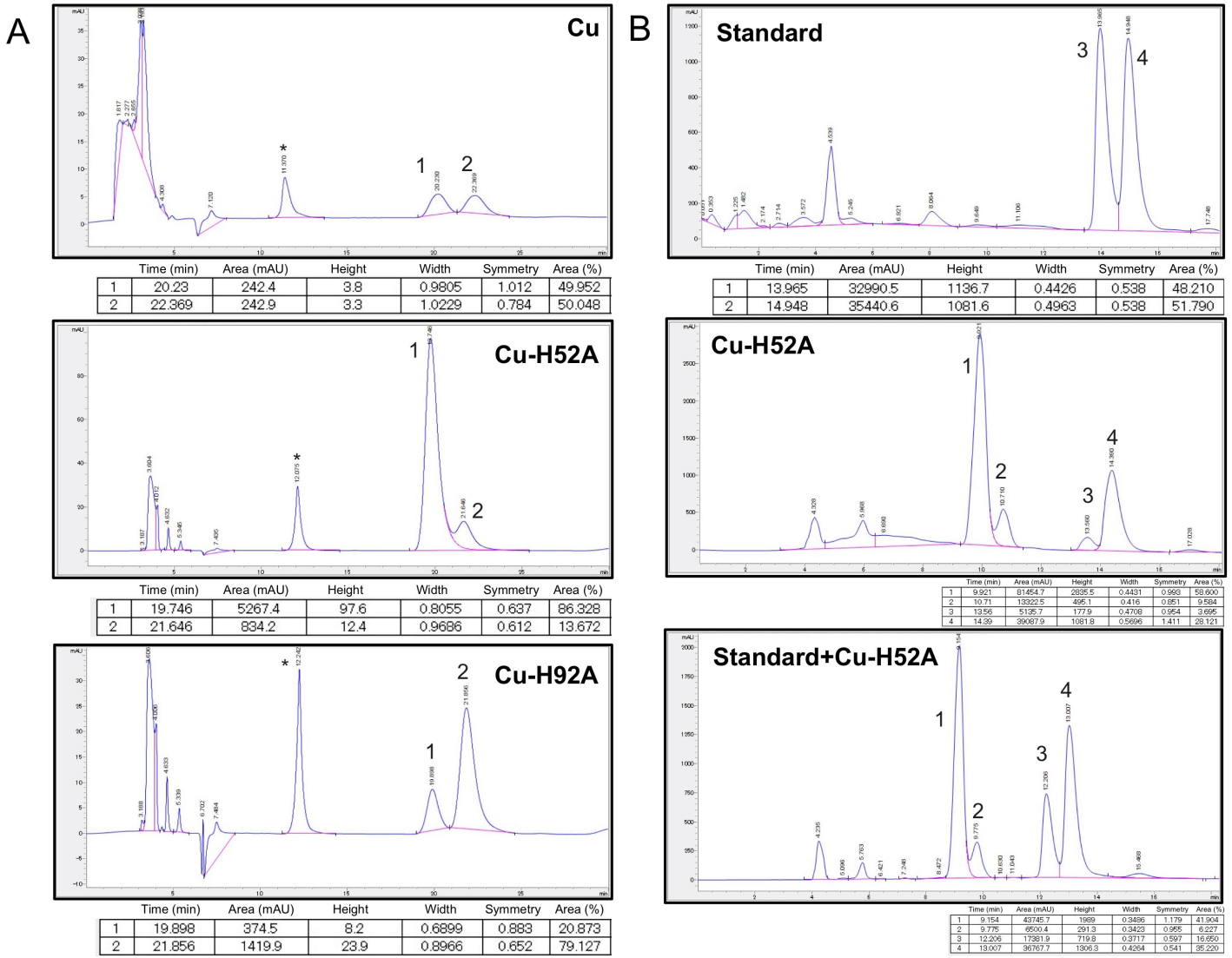

Figure S3. Separation of product stereoisomers for the Michael addition of methyl acetoacetate and dimethyl malonate catalyzed by selected mutant on chiral normal-phase chromatography. (A) Separation of product **2**, 1, (*R*)-(–)-isomer; 2, (*S*)-(+)- isomer. (B) Separation of product **2** and its *N*-oxide **2'**, 1 (*R*)-(–)-isomer; 2, (*S*)-(+)-isomer; 3, (*S*)-(+)-*N*-oxide; 4, (*R*)-(–)-*N*-oxide. See SI Experimental.

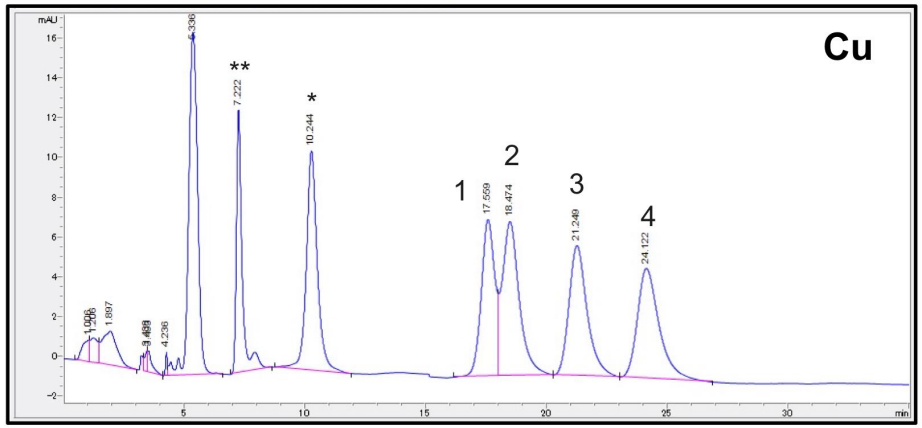

	Time (min)	Area (mAU)	Height	Width	Symmetry	Area (%)
1	17.559	305.6	7.8	0.5822	0.975	22.304
2	18.474	375.3	7.7	0.7067	0.76	27.394
3	21.249	341.5	6.5	0.7662	0.742	24.930
4	24.122	347.6	5.5	0.9095	0.653	25.372

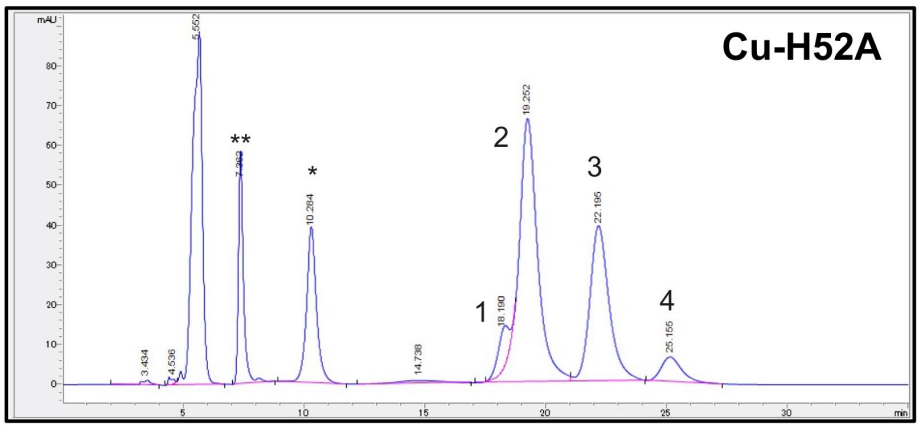

	Time (min)	Area (mAU)	Height	Width	Symmetry	Area (%)
1	18.19	339	10	0.4906	0.832	5.219
2	19.252	3630.2	65.6	0.8694	1.401	55.886
3	22.195	2166.1	38.4	0.8825	0.82	33.347
4	25.155	360.4	6.1	0.9413	0.736	5.548

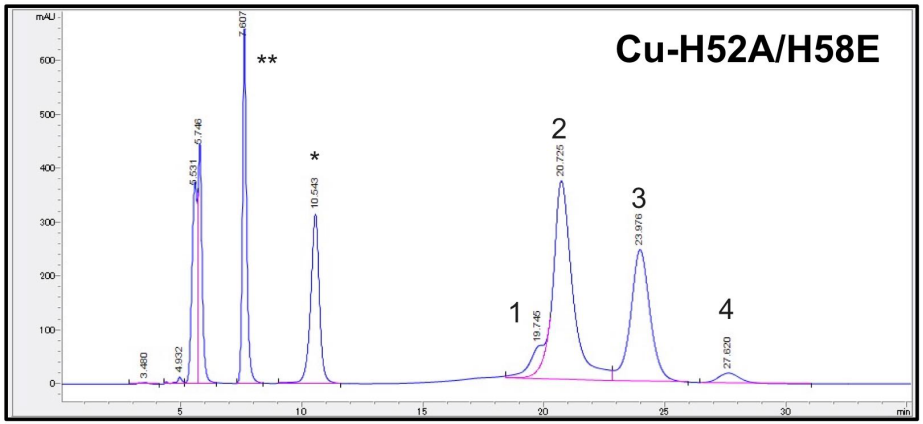

	Time (min)	Area (mAU)	Height	Width	Symmetry	Area (%)
1	19.745	2031.1	44.7	0.6345	2.042	5.360
2	20.725	21074.4	367.9	0.8364	1.133	55.613
3	23.976	13718.3	243.7	0.8408	0.922	36.201
4	27.62	1071.2	18.3	0.9061	0.909	2.827

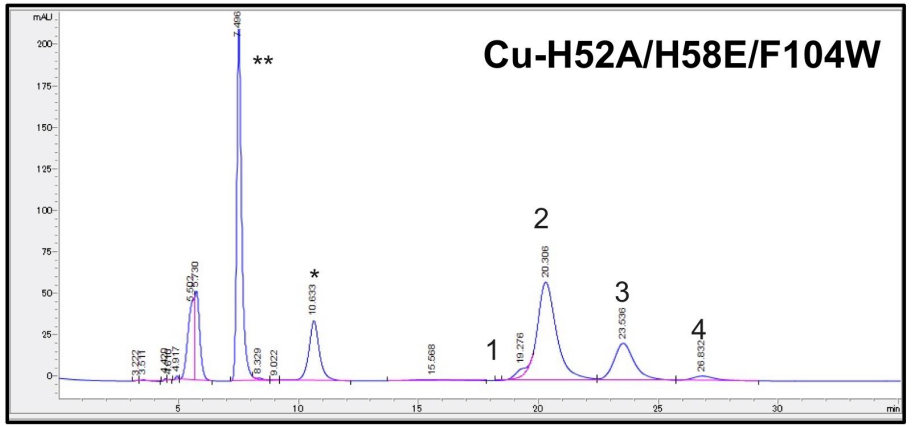

	Time (min)	Area (mAU)	Height	Width	Symmetry	Area (%)
1	19.276	159.6	4.8	0.4796	1.36	3.146
2	20.306	3426.8	59.1	0.8546	0.975	67.558
3	23.536	1322.5	22.3	0.8873	0.796	26.073
4	26.832	163.5	2.6	0.8412	0.753	3.223

Figure S4. Separation of product stereoisomers for the Michael addition of methyl acetoacetate and dimethyl malonate catalyzed by selected mutant on chiral normal-phase chromatography. Separation of product **3**, 1, (+)-*anti*-isomer; 2, (–)-*anti*-isomer; 3, (–)-*syn*-isomer; 4, (+)-*syn*-isomer.

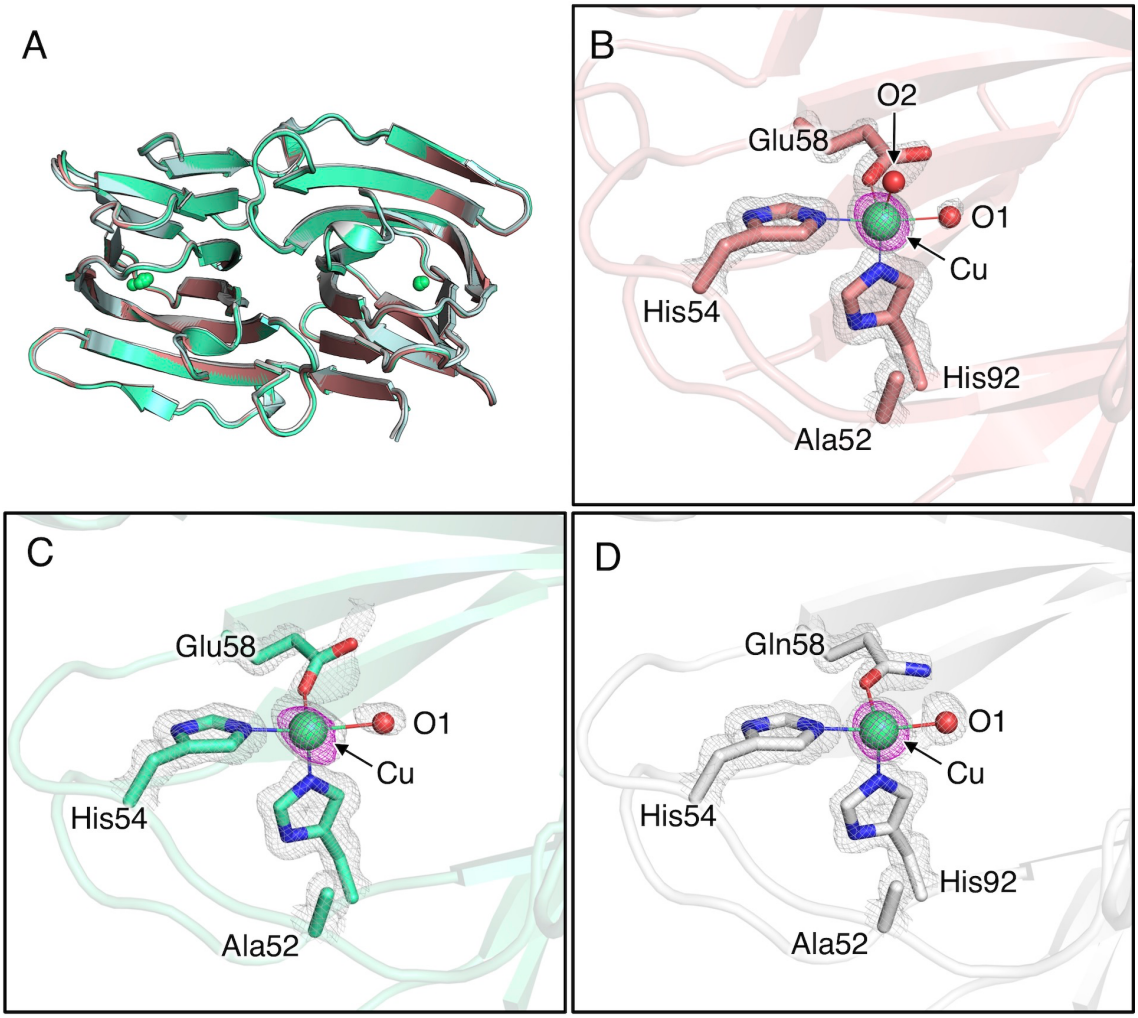

Figure S5. The crystal structure of Cu-bound H52A/H58E (pink, PDB code: 8HJX), Cu-bound H52A/H58E/F104W (green, PDB code: 8HJY) and Cu-bound H52A/H58Q (white, PDB code: 8HJZ). (A) Superimposed overall structures of Cu-bound H52A (blue), H52A/H58E, H52A/H58E/F104W and H52A/H58Q, (B) Cu-binding site of H52A/H58E (Chain A), (C) Cu-binding site of H52A/H58E/F104W (Chain A), (D) Cu-binding site of H52A/H58Q (Chain A). The 2*F*o-*F*c and anomalous maps are contoured at 1.5 and 5.0 and shown in gray and magenta mesh, respectively.

The copper content of Cu-bound H52A/H58E, Cu-bound H52A/H58E/F104W and Cu-bound H52A/H58Q were determined to be 1.1, 0.9 and 1.0 per protein subunits, respectively, by the ICP-AES analysis. Overall structures of Cu-bound H52A/H58E was almost the same to that of the Cu-bound H52A (H52A/H58E vs. H52A, rmsd = 0.268 Å, 228 Cα). Overall structures of Cu-bound H52A/H58E/F104W and Cu-bound H52A/H58Q are almost the same to that of the Cu-bound H52A/H58E (H52A/H58E/F104W vs. H52A/H58E, rmsd = 0.154 Å, 228 Cα; H52A/H58Q vs. H52A/H58E, rmsd = 0.210 Å, 228 Cα). In the Cu binding site of H52A/H58E, His54 and His92 coordinate to Cu at cis position in the equatorial plane with two water molecules (O1 and O2, Figure S5B), whereas the water molecule O2 was not seen in either H52A/H58E/F104W or H52A/H58Q. In the chain B of H52A/H58E, the minor copper species (Cu(B), their occupancy is 37 %) were observed in the proximity of major copper species (Cu(A), their occupancy is 47 %) within the distance of 0.54 ± 0.02 Å (Figure 2A).

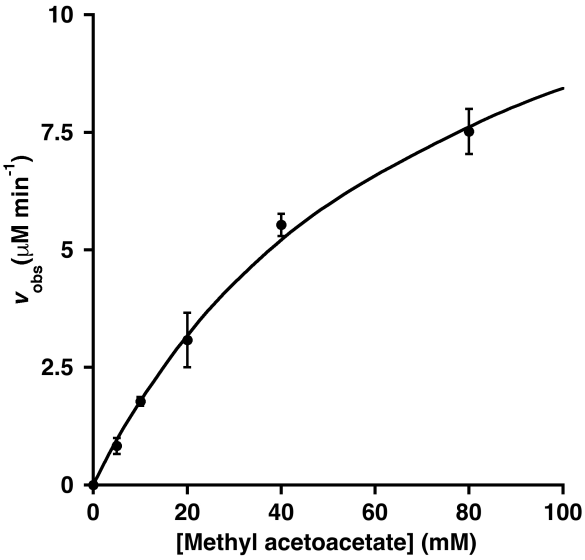

Figure S6. Michaelis-Menten saturation kinetics of H52A/H58E/F104W mutant upon copper addition for the Michael addition of methyl acetoacetate (5-80 mM) to azachalcone (5 mM) in potassium phosphate-buffer (pH 6.5, 20 mM, 20 °C). An analysis based on the Michaelis-Menten mechanism provides a good fit with the following catalytic turnover number and Michaelis constant: k_{cat} = 0.093 min^{-1} and K_M = 66 mM.

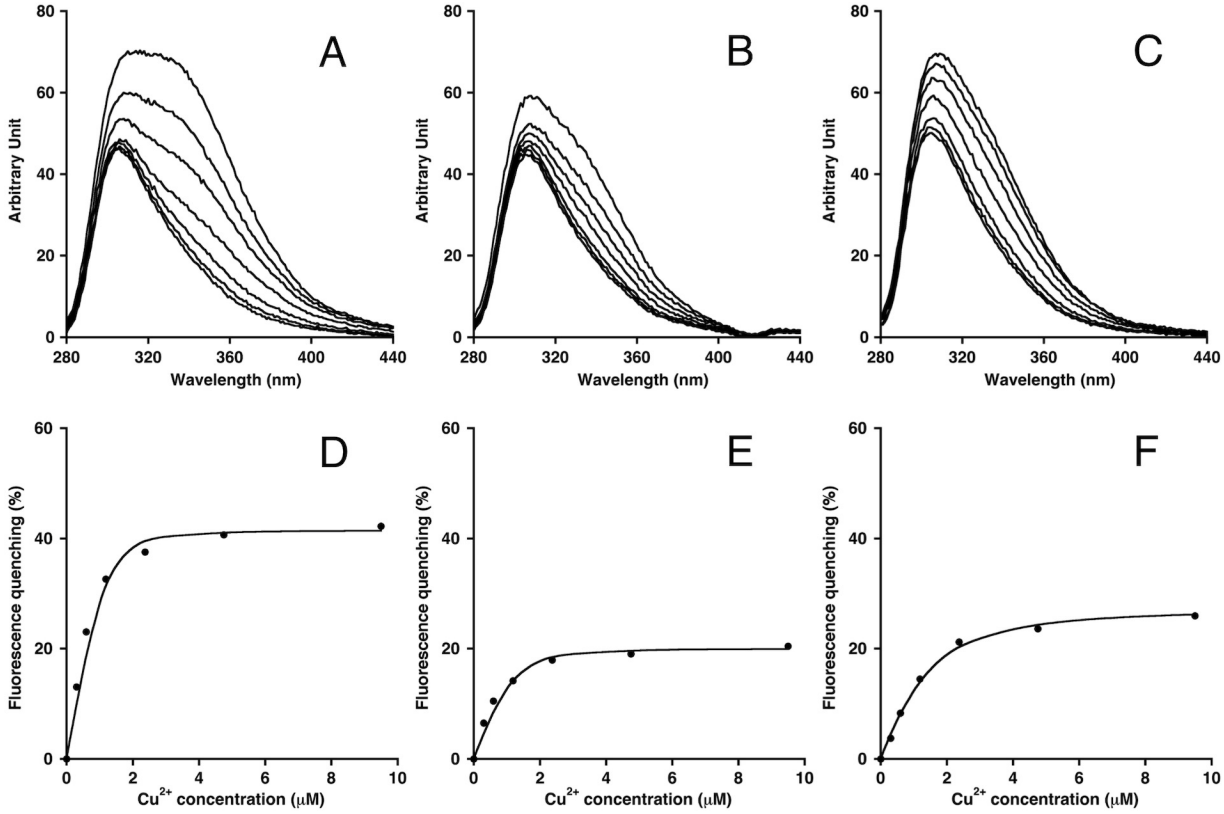

Figure S7. Fluorescence spectral changes observed during the titration of TM1459 mutants (0.12 μM) with aliquots of $CuSO_4$ at 25 °C and pH 7.0 (20 mM potassium phosphate). Background subtracted 265 nm-excited fluorescence emission spectra of TM1459 mutants (A, H52A; B, H52A/H58E; C, H52A/H58Q) upon addition of $CuSO_4$ (0, 0.3, 0. 6. 1.2, 2.4, 4.8, and 9.5 μM, top to bottom). Fluorescence quenching profile at 331 nm (in %) resulting from addition of $CuSO_4$ to TM1459 mutants (D, H52A; E, H52A/H58E; F, H52A/H58Q). Analysis based on a one metal binding scheme provides a good fit with the following dissociation constants: K_d (H52A) = 0.053 μM, K_d (H52A/H58E) = 0.11 μM, and K_d (H52A/H58Q) = 0.53 μM. The corresponding fluorescence quenching values (ΔF) for H52A, H52A/H58E, H52A/H58Q variants are 42, 20, and 28 %, respectively.

A

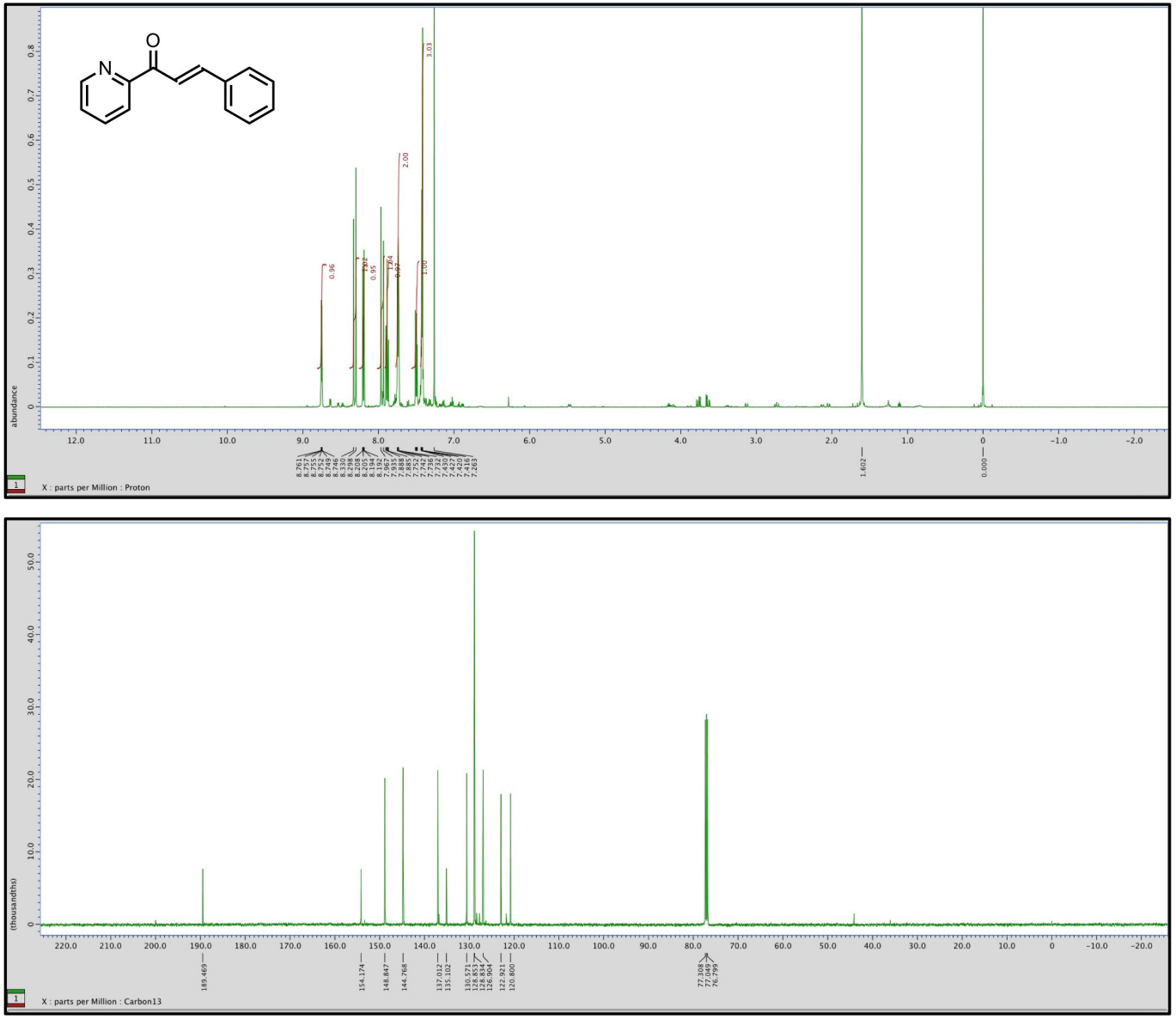
O
N
abundance
X : parts per Million : Proton
(thousandths)
X : parts per Million : Carbon13

B

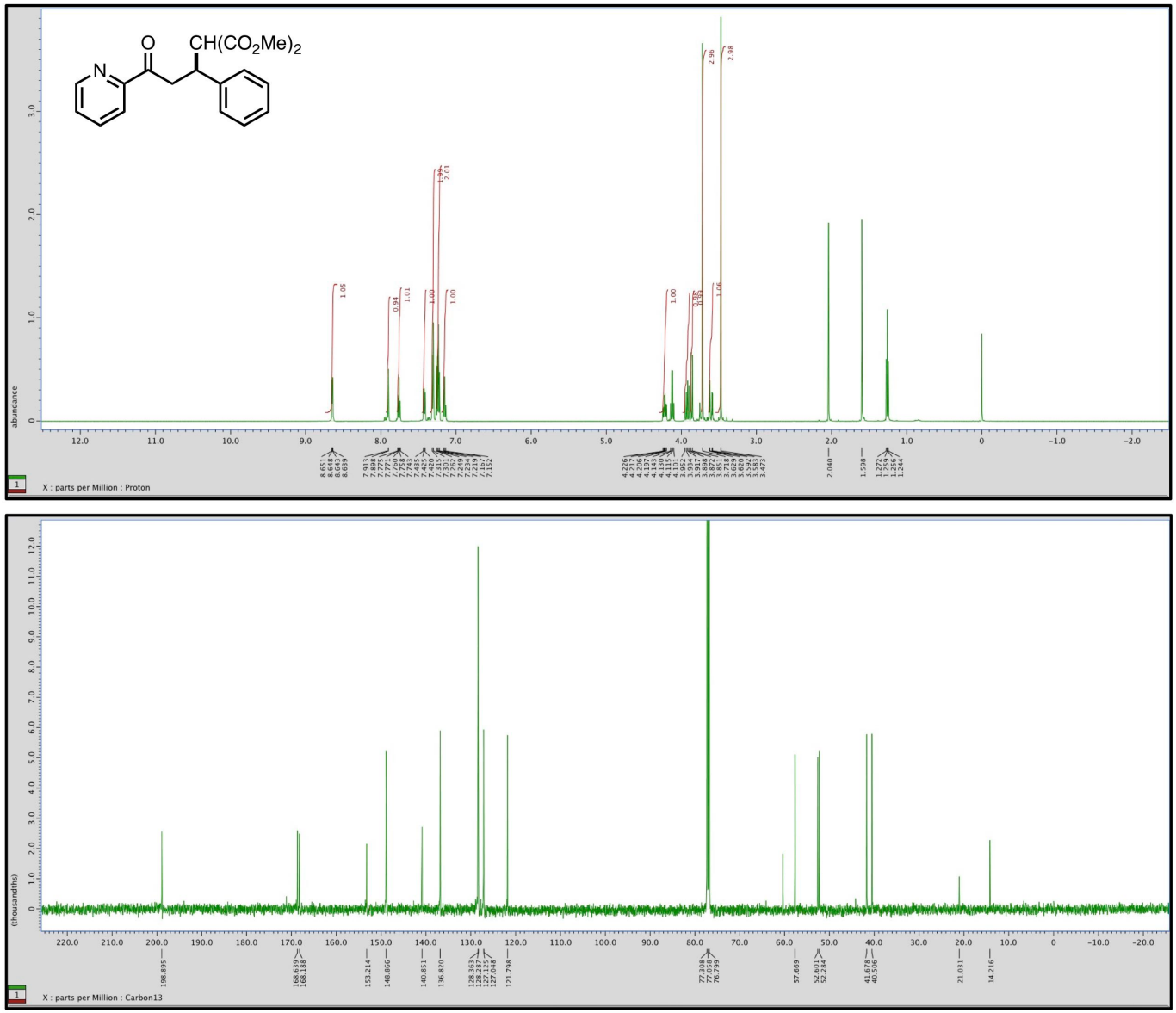
O
CH(CO2Me)2
N
abundance
X : parts per Million : Proton
(thousandths)
X : parts per Million : Carbon13

C

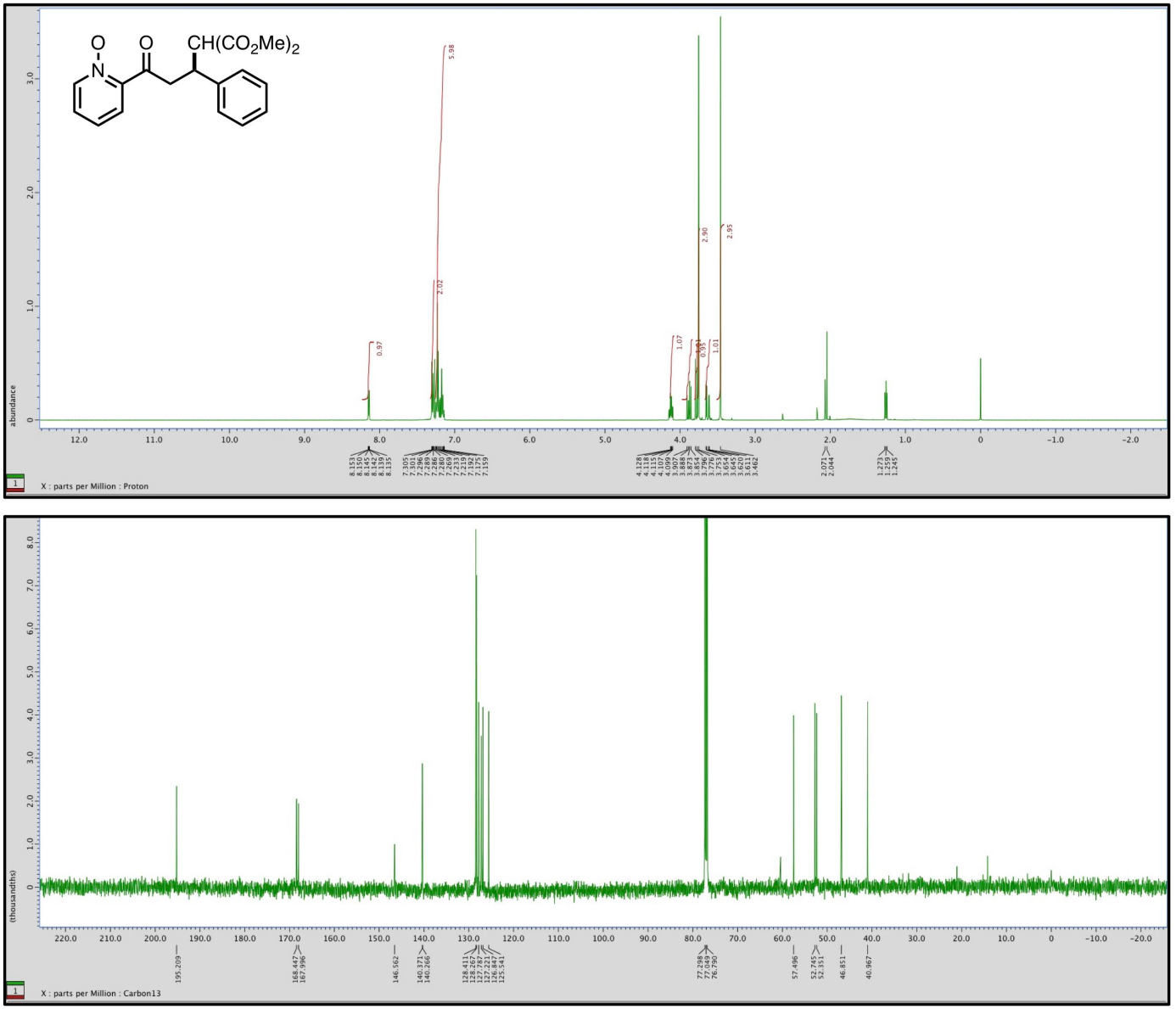
O
O
N
CH(CO2Me)2
abundance
X : parts per Million : Proton
(thousandths)
X : parts per Million : Carbon13

D

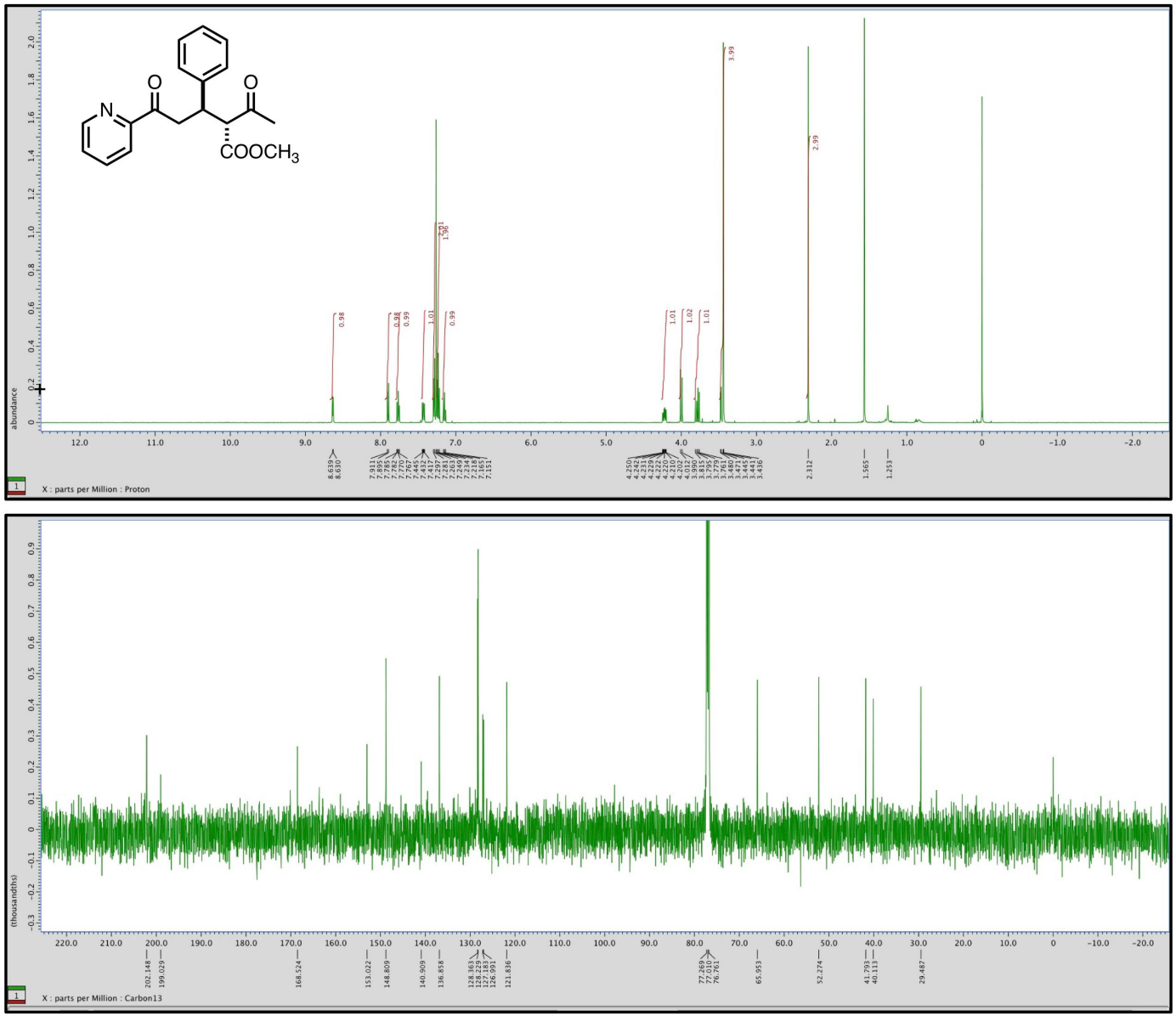
O
N
O
COOCH3
abundance
X : parts per Million : Proton
(thousandths)
X : parts per Million : Carbon13

E

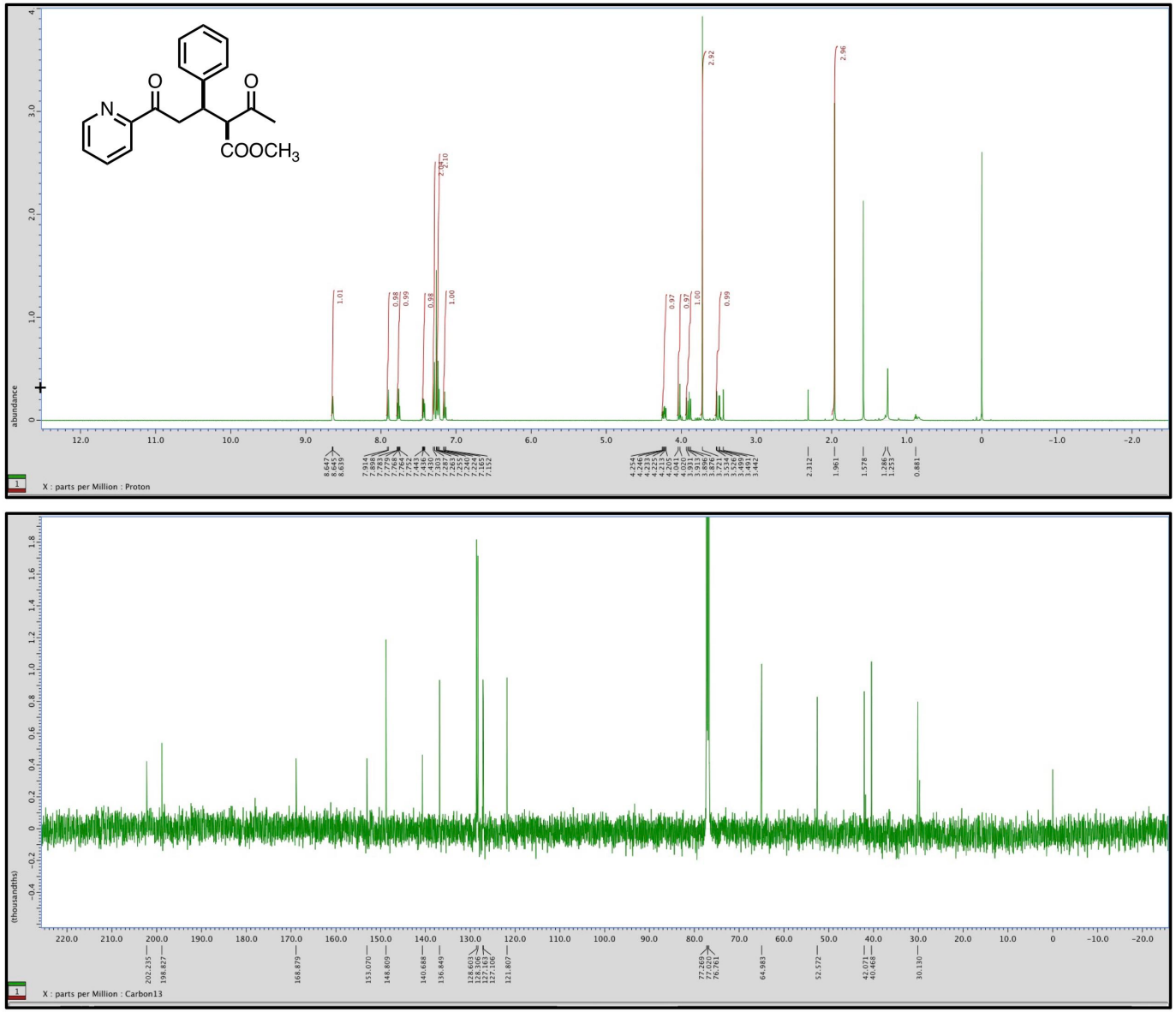

Figure S8. NMR data of the compounds studied in this study.